

# X-Light: Cross-City Traffic Signal Control Using Transformer on Transformer as Meta Multi-Agent Reinforcement Learner

Haoyuan Jiang<sup>1\*</sup>, Ziyue Li<sup>2,†</sup>, Hua Wei<sup>3</sup>, Xuantang Xiong<sup>4\*</sup>, Jingqing Ruan<sup>4\*</sup>, Jiaming Lu<sup>5\*</sup>, Hangyu Mao<sup>6</sup> and Rui Zhao<sup>6,7</sup>

<sup>1</sup>Baidu Inc., China

<sup>2</sup>University of Cologne, Germany

<sup>3</sup>Arizona State University, U.S.A

<sup>4</sup>Institute of Automation, Chinese Academy of Sciences, China

<sup>5</sup>Fudan University, China

<sup>6</sup>SenseTime Research, China

<sup>7</sup>Qingyuan Research Institute, China

jianghaoyuan@zju.edu.cn, zlibn@wiso.uni-koeln.de.

## Abstract

The effectiveness of traffic light control has been significantly improved by current reinforcement learning-based approaches via better cooperation among multiple traffic lights. However, a persisting issue remains: how to obtain a multi-agent traffic signal control algorithm with remarkable transferability across diverse cities? In this paper, we propose a **Transformer on Transformer (TonT)** model for *cross-city* meta multi-agent traffic signal control, named as X-Light: We input the full Markov Decision Process trajectories, and the Lower Transformer aggregates the states, actions, rewards among the target intersection and its neighbors *within a city*, and the Upper Transformer learns the general decision trajectories *across different cities*. This dual-level approach bolsters the model’s robust generalization and transferability. Notably, when directly transferring to unseen scenarios, ours surpasses all baseline methods with **+7.91%** on average, and even **+16.3%** in some cases, yielding the best results. The code is [here](#).

## 1 Introduction

An effective traffic signal control (TSC) system is the key to alleviating traffic congestion. In recent years, Reinforcement Learning (RL) has been widely used in the field of TSC [Yau *et al.*, 2017]. It can interact with the environment, explore, and exploit, which helps agents discover better policies without artificial priors and assumptions. Numerous studies [Wei *et al.*, 2019a; Zheng *et al.*, 2019; Chen *et al.*, 2020; Wei *et al.*, 2019b; Chu *et al.*, 2019; Lu *et al.*, 2023; Du *et al.*, 2024] have demonstrated its noteworthy enhancements over conventional rule-based methods [Hunt *et al.*, 1982; Lowrie, 1990; Roess *et al.*, 2004].

However, most of the existing methods are *scenario-specific*, meaning that the training and testing should be in the same scenario (A scenario is a simulation environment, e.g., a virtual city, with a set of intersections). When deploying on a new scenario, rebuilding the environment and re-training are needed, which involves significant costs. As a result, to the best of our knowledge, all the cities still use rule-based methods such as SCATS or SCOOT for a very fundamental reason: they can be easily reused in a new district/region/city.

This raised a critical problem that **how to orchestrate the multiple intersections for various scenarios/cities with strong generalizability**.

There are some solutions for single-agent setting: MetaLight [Zang *et al.*, 2020] and GESA [Jiang *et al.*, 2024] used one single agent to control all the intersections in a scenario and achieve transferability via gradient-based meta RL and multi-city co-training, respectively. Their drawbacks are obvious, i.e., neglecting the cooperation among the multiple intersections. Yet, learning a general Multi-Agent RL model for various scenarios is non-trivial, given various scenarios could have various road networks and traffic dynamics, rendering various environment states for each agent and collaboration patterns for multiple agents. To the best of our knowledge, only a few existing works target the same challenge: MetaVIM [Zhu *et al.*, 2023] and MetaGAT [Lou *et al.*, 2022]. They both utilized the Markov Decision Processes (MDPs) trajectories to help the agents learn and distinguish scenario context. However, they still display limitations, such as an unstable training process and large performance drops when encountering quite dissimilar scenarios (details in Sec. 2).

To enhance cooperation and generalizability, we will incorporate the full MDP trajectories, including the observations, rewards, and actions ( $o, a, r$ ) of both the target intersection and its neighbors, into the method. Given the sequence nature of the trajectories from various MDPs, two natural questions are: **Q1: Can Transformer utilize the  $o, a, r$  sequences of multiple intersections for better collaboration?** **Q2: Furthermore, can we Transformer learn the high-level cross-scenario MDPs dynamics for better transfer-**

\*Research mainly done when with SenseTime Research

†Corresponding Author

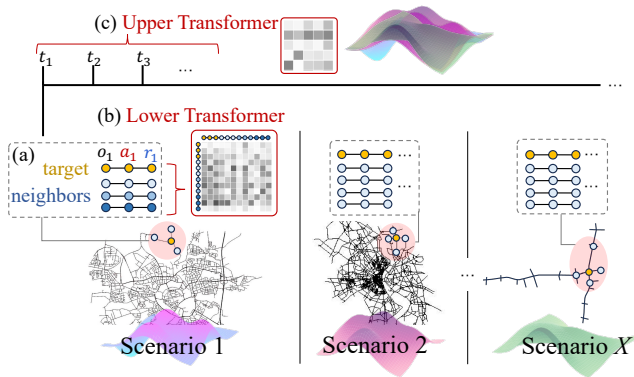


Figure 1: (a) X-Light takes the MDP  $o, a, r$  trajectories of the target and its neighbors: (b) the Lower Transformer learns the attention for all the  $o, a, r$ -s, so that, e.g., one intersection’s  $o$  may have high attention with another intersection’s  $a$ ; (c) Upper Transformer learns the attention over the time through all different scenarios.

**ability.** This forms our solution as in Figure 1: a Transformer on Transformer (TonT) model for Meta Multi-Agent Reinforcement Learners. The **Lower Transformer** extracts single-step trajectory information from the target intersection and its neighbor intersections to encourage cooperation. The **Upper Transformer** learns from the historical multi-scenario multi-modal MDPs distributions and makes actions.

The main contributions are three-fold:

- In the domain of TSC, we propose the first-ever Transformer-on-Transformer (TonT) framework for meta MARL, which solves both multi-intersection collaboration and cross-city transferability/generalizability.
- Specifically, the **Lower Transformer** aggregates the target and its neighbors’ fine-grained  $o, a, r$  information and achieves better collaboration than other solutions such as the Graph Neural Network (GNN)-based methods [Wei *et al.*, 2019b; Lou *et al.*, 2022], which only aggregates traffic states  $o$ ; The **Upper Transformer**, together with a *dynamic prediction* pretext task and *multi-scenario co-training scheme*, learns the scenario-agnostic decision process and achieves better cross-city decision. Additionally, a *residual link* is added before inputting to actor-critic for better decision.
- We conduct rigid experiments with various scenarios and zero-shot transfer to each, and our method is constantly the best performer. In non-transfer settings, we also achieve the most top one results.

## 2 Related Work

### 2.1 Meta Reinforcement Learning-based TSC

Meta RL-based methods are gaining attention in TSC since they can greatly reduce adaptation costs and have promising performance in new scenarios. GeneralLight [Zhang *et al.*, 2020] and AttendLight [Oroojlooy *et al.*, 2020] try to generalize TSC to different traffic flow patterns: they use GAN [Goodfellow *et al.*, 2014] and two attention models to handle traffic diversity. However, it is not strictly adapting to a new

scenario. MetaLight [Zang *et al.*, 2020] can be seen as the pioneering work of training a TSC agent in multiple scenarios: it uses gradient-based meta-reinforcement learning with base function reading each local data and updating local gradients, and meta-learner accumulating the memory and updating the global gradients. GESA [Jiang *et al.*, 2024] instead proposed a general plug-in module (GPI) to make it possible to read various cities’ maps without labels and further uses large-scale scenarios to co-train an actor-critic-based agent. But all of them only considered single-agent settings and ignored the cooperation with others. However, to model the cooperative multi-agent under multiple various scenarios is quite technically challenging. Only a few models are proposed, yet their performance is quite unstable and limited.

MetaVIM [Zhu *et al.*, 2023] uses context-based Meta RL to solve the generalization problem and uses intrinsic rewards to cooperate, but it is only trained in one scenario and the state does not contain neighbor information, leading to challenges in performance and adaptability when encountering an environment that is different from the training scenario. MetaGAT [Lou *et al.*, 2022] extends MetaLight with a Graph Attention Network (GAT) to aggregate the neighbors’ observations into the target’s and Gated Recurrent unit (GRU) to learn the MDP dynamics. However, it has volatile fluctuations during the training process and suboptimal performance. Potential reasons are that (1) it is trained with one scenario after another, but we mix intersections from various scenarios within one batch; (2) Relying on GAT restricts them to only utilize observation information as node feature, overlooking crucial actions and rewards within the MDP. We instead use Lower Transformer to fully construct the relation among  $o, a, r$  from multiple intersections; (3) A hybrid model of combining GAT and GRU may be harder to train, and we are an elegant, Transformer-only model.

### 2.2 Transformers in RL and Other Fields

**Offline RL** unfolds the MDP process as a sequence of  $s_t, a_t, r_t, s_{t+1}$  etc. Thus, works such as Decision Transformer (DT) [Chen *et al.*, 2021], PDiT [Mao *et al.*, 2023], and Trajectory Transformer (TT) [Janner *et al.*, 2021] use Transformer as the backbone, treating decision-making as a next-token prediction, i.e., to predict the next action  $a_{t+1}$ . TransformerLight [Wu *et al.*, 2023] got inspired by DT and trained a TSC agent with offline-collected data. However, training with offline-collected data means a heavy workload to prepare high-quality data, and it cannot interact with the environment in real-time, let alone transfer to a new scenario. To increase transferability, PromptDT [Xu *et al.*, 2022] proposes to add few-shot task-specific sequences as the prompt for quick adaptation for new tasks. However, offline data is still needed.

**Transformer as Meta RL:** TrMRL [Melo, 2022] is the pioneering work that proves Transformer can function as a meta-agent. Similar to the memory reinstatement mechanism, this agent establishes connections between the immediate working memories to construct an episodic memory across the transformer layers iteratively. Our work is the first one that applies a Transformer-based meta agent into the TSC domain; we further extend the original single-agent setting to

multi-agent, with several technical challenges overcome by our final TonT solution: the Lower Transformer guides cooperation with neighbors utilizing  $o, a, r$  information, and the upper Transformer learns meta-features across tasks, showcasing remarkable generalization capabilities.

### 3 Methodology

This section delineates our proposed method, X-Light, a general cross-city multi-agent traffic signal control method. We begin by providing an overview of our method, followed by the introduction of the TonT Encoder module, which contains the Lower Transformer and the Upper Transformer. Finally, we will give detailed settings for training. The preliminary information is presented in the Appx. A.

#### 3.1 Overview

As shown in Fig. 2, our method is trained using intersections across various scenarios within a batch. The  $i$ -th intersection and its neighbors  $\mathcal{N}_i$  are selected, and their MDP trajectories  $(o, a, r)$  from time frame  $[t - K + 1, t]$  are sampled and fed into TonT Encoder module. It is worth noting that to allow the model to handle various intersections, we use the GPI module proposed in [Jiang *et al.*, 2024], which maps various intersections' structure into a unified one, followed by an MLP to obtain  $o_t^{\{i, \mathcal{N}_i\}}$ . More details are in the Appx. C.

As shown in Fig. 2, the TonT Encoder employs two types of transformers: the Lower Transformer and the Upper Transformer. The primary role of the Lower Transformer is to integrate the target and its neighbors' MPD information at time step  $t$ . It enhances agent collaboration compared with GNN-based collaboration by 6%-13%. The Upper Transformer utilizes historical trajectory information as context to infer the current task, thereby achieving improved transferability.

The output of the TonT Encoder is then utilized by both the Actor and Critic to output the policy  $\pi$  for executing the action and to estimate the state value for training.

Similar to [Wei *et al.*, 2021], we choose five features from the observations as states: queue length, current phase, occupancy, flow, and the number of stopping cars. The action is to choose the eight pre-defined phases for the next time interval, as shown in Fig 2. At each time step  $t$ , the agent  $i$  can choose to execute action  $a_t^i$  from available action set  $\mathcal{A}^i$  in the next  $\Delta t$  seconds. In our experiments, we set  $\Delta t$  as 15 seconds. The reward  $r$  is defined as the weighted sum of queue length, wait time, delay time, and pressure. More details in Appx. C.

#### 3.2 Lower Transformer

The Lower Transformer enhances collaboration between the target  $i$  and its  $n$ -nearest neighbors  $\mathcal{N}_i, \mathcal{N}_i = \{N_1, \dots, N_n\}$ . Existing multi-agent TSC methods only consider the states of neighboring intersections for cooperation, neglecting the complex and valuable interrelations among their observations, actions, and rewards. Considering the variations in road networks and traffic flow interconnections across diverse scenarios, one intersection's action will affect another's state and also vice versa. Thus, only relying on states is inadequate to simulate the neighbors' impacts on the target accurately. This can further result in instability within the learning process,

especially during cross-scenario co-training, as we observed in MetaLight and MetaGAT's training process.

Thus, in the Lower Transformer, we utilize the **full** MDP features of the target and its neighbors to enhance the model's understanding of the cooperation. Since we are online RL, at time  $t$ , we can only observe immediate  $o_t$  and the previous step's  $a_{t-1}, r_{t-1}$ . Thus, the  $i$ th agent's MDP feature at  $t$  is:

$$\mathbf{m}_t^i = (\mathbf{o}_t^i, \mathbf{a}_{t-1}^i, \mathbf{r}_{t-1}^i) \quad (1)$$

Since original  $\mathbf{o}, \mathbf{a}, \mathbf{r}$  have different dimensions, we first employ three trainable linear projections, i.e.,  $\mathbf{E}_o, \mathbf{E}_a, \mathbf{E}_r$ , to map all of them to the same dimension of  $d$ . Then, the full MDP transition with neighbors concatenated is defined as:

$$\mathbf{M}_t^i = [\mathbf{m}_t^i \mathbf{E}; \mathbf{m}_t^{N_1} \mathbf{E}; \dots, \mathbf{m}_t^{N_n} \mathbf{E}] \in \mathbb{R}^{3(1+n) \times d} \quad (2)$$

where  $\mathbf{m}_t^i \mathbf{E} = (\mathbf{o}_t^i \mathbf{E}_o, \mathbf{a}_{t-1}^i \mathbf{E}_a, \mathbf{r}_{t-1}^i \mathbf{E}_r) \in \mathbb{R}^{3 \times d}$

If the number of neighbors is smaller than  $n$ , we use zero-padding and add a binary indicator embedding to all  $\mathbf{o}_t$  to indicate whether this neighbor exists.

Similar to ViT [Dosovitskiy *et al.*, 2020], a learnable `[class]` token is prepended serving as the global image representation, we also prepend a trainable `[decision]` token  $\mathbf{q}_{\text{decision}} \in \mathbb{R}^d$ , whose state at the output of the Lower Transformer is used as the intersection representation  $\mathbf{c}_t$ . We also add standard position embedding [Vaswani *et al.*, 2017] to each input token to retain positional information. Thus, the input to the Lower Transformer  $\mathbf{z}_{t,i}^{\text{lower}}$  is:

$$\mathbf{z}_{t,i}^{\text{lower}} = [\mathbf{q}_{\text{decision}}; \mathbf{m}_t^i \mathbf{E}; \mathbf{m}_t^{N_1} \mathbf{E}; \dots, \mathbf{m}_t^{N_n} \mathbf{E}] + \mathbf{E}_{\text{pos}}^{\text{lower}} \quad (3)$$

where  $\mathbf{z}_{t,i}^{\text{lower}}, \mathbf{E}_{\text{pos}}^{\text{lower}} \in \mathbb{R}^{(3(1+n)+1) \times d}$  and the attention in the Lower Transformer is in  $\mathbb{R}^{(3(1+n)+1) \times (3(1+n)+1)}$ . Then, we feed  $\mathbf{z}_{t,i}^{\text{lower}}$  to the Lower transformer with 3 multi-head self-attention layers, and it outputs a capsulized intersection embedding for further decision-making, denoted as  $\mathbf{c}_t^i$ .

$$\mathbf{c}_t^i = \text{Lower Transformer}(\mathbf{z}_{t,i}^{\text{lower}}) \quad (4)$$

#### 3.3 Upper Transformer

The Upper Transformer ensures that the model exhibits strong generalization in the presence of unseen intersections or scenarios. To achieve this goal, as shown in Fig. 2.(b2), we employ *context-based meta RL* [Duan *et al.*, 2017] and a *dynamic predictor* within the Upper Transformer.  $\mathbf{c}_{[t-K+1:t]}^i$  obtained from the Lower Transformer is first projected to dimension- $d'$  through a trainable projection denoted as  $\mathbf{E}'$ . Then, as the context-based meta RL, the Upper Transformer utilizes these embeddings from the last  $K$  time steps. Similarly, along with the positional embedding, the input to the Upper Transformer is  $\mathbf{z}_{[t-K+1:t],i}^{\text{upper}} \in \mathbb{R}^{K \times d'}$ :

$$\mathbf{z}_{[t-K+1:t],i}^{\text{upper}} = [\mathbf{c}_{t-K+1}^i \mathbf{E}'; \mathbf{c}_{t-K+2}^i \mathbf{E}'; \dots; \mathbf{c}_t^i \mathbf{E}'] + \mathbf{E}_{\text{pos}}^{\text{upper}}, \quad (5)$$

The attention mechanism in the Upper Transformer (consisting of 3 multi-head self-attention layers) operates within the  $\mathbb{R}^{K \times K}$  dimension, capturing the environmental dynamics related to the target intersection from historical features.

$$\mathbf{z}_{[t-K+1:t],i}^{\text{output}} = \text{Upper Transformer}(\mathbf{z}_{[t-K+1:t],i}^{\text{upper}}) \quad (6)$$

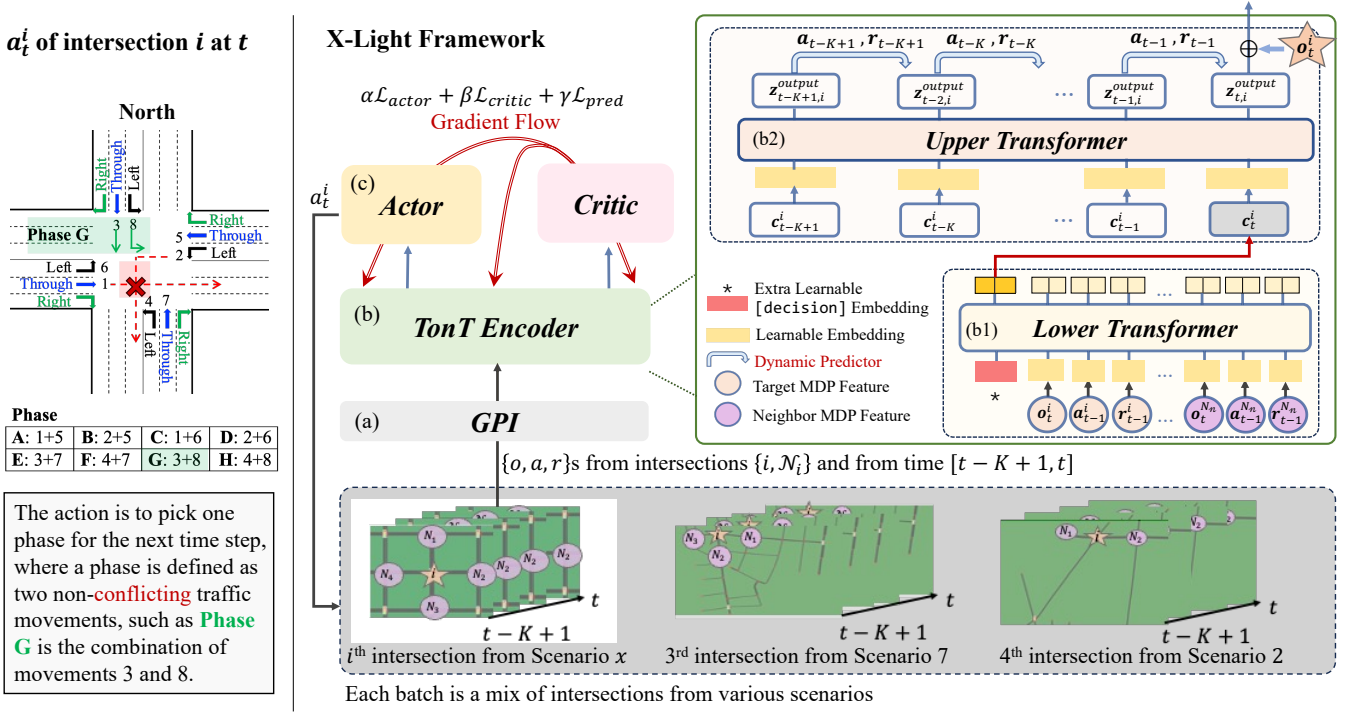


Figure 2: Our method is co-trained with intersections’ MDPs from various scenarios: (a) a GPI module unifying all the scenarios, (b) the proposed TonT Encoder, and (c) an actor-critic to make a decision. The TonT Encoder contains (b1) a Lower Transformer aggregating the  $o$ ,  $a$ , and  $r$  among the target and its neighbors and (b2) an Upper Transformer learning general decisions from multi-scenario historical MDPs.

**Dynamic Predictor:** To enhance the agent’s comprehension of the current task and the influence between intersections, we introduce a dynamic predictor between the Upper Transformer’s each time-step output, enhancing the agent to learn the environment dynamics. The dynamic predictor is a pretext prediction task to conduct autoregression prediction, encouraging the Upper Transformer to capture the cross-scenario dynamics. As shown in Fig. 4, this dynamic predictor can improve performance by 4.4%. Specifically, we feed the previous time step  $\mathbf{z}_{t-1,i}^{\text{output}}$  concatenated with all the actions  $\mathbf{a}_{t-1}^{\{i, \mathcal{N}_i\}}$  and rewards  $\mathbf{r}_{t-1}^{\{i, \mathcal{N}_i\}}$  from the target and its neighbors, to predict the next  $\mathbf{z}_{t,i}^{\text{output}}$ :

$$\hat{\mathbf{z}}_{t,i}^{\text{output}} = \text{MLP}([\mathbf{z}_{t-1,i}^{\text{output}}; \mathbf{a}_{t-1}^{\{i, \mathcal{N}_i\}}; \mathbf{r}_{t-1}^{\{i, \mathcal{N}_i\}}]) \quad (7)$$

A prediction loss based on mean squared error (MSE) is:

$$\mathcal{L}_{pred} = \text{MSE}(\hat{\mathbf{z}}_{t,i}^{\text{output}}, \mathbf{z}_{t,i}^{\text{output}}) \quad (8)$$

### 3.4 Actor-Critic

For the decision policy  $\pi$ , we use the PPO method [Schulman *et al.*, 2017], both Actor and Critic are two-layer MLPs. The actor receives the TonT Encoder’s output and makes the action  $a_t^i$  for the target intersection  $i$ .

**Residual Link:** However, before inputting into the actor-critic module, to avoid over-abstracting the intersection’s embedding through the TonT Encoder, we directly add the observation  $o_t^i$  of the target intersection  $i$  into the Upper Transformer’s output  $\mathbf{z}_{t,i}^{\text{output}}$ . This ensures the embedding input into

the actor has enough observational information from the target intersection.

$$\mathbf{a}_t^i \sim \pi(\cdot | \mathbf{z}_{t,i}^{\text{output}} + o_t^i) \quad (9)$$

The  $\mathbf{z}_{t,i}^{\text{output}}$  is the embedding after TonT Encoder’s feature abstraction, which is particularly essential for scenarios with complex intercorrelations;  $o_t^i$  instead is the direct self-observation, which is proven as rather essential for simple scenarios, where focusing on yourself is enough. As shown in Fig.4, without residual link can lead to a 2% performance drop. Thus, our design strikes a good balance for scenarios in various complexity. Therefore, together with Eq. (8), the overall optimization objective can be formatted as:

$$\mathcal{L} = \alpha\mathcal{L}_{actor} + \beta\mathcal{L}_{critic} + \gamma\mathcal{L}_{pred}, \quad (10)$$

where  $\alpha, \beta, \gamma$  are tuning parameters. The Actor loss and Critic loss are the same as PPO.

### 3.5 Multi-scenario Co-Training

To further increase model generality, we employed the multi-scenario co-train to increase data diversity. Unlike MetaGAT [Lou *et al.*, 2022] or MetaLight [Zang *et al.*, 2020], which utilizes the multi-scenario sequential training, i.e., within a batch, intersections are from the same scenario, and scenarios are read until previous one is all seen, we adopted multi-scenario co-training, i.e., within each batch, intersections are stochastically chosen from various scenarios. Given each intersection from each scenario has a distinct structure, we adopt a general preprocess module, GPI

---

**Algorithm 1** X-Light training process

---

**Input:** A set of target intersections  $\mathcal{I}$  from a set of multi-agent scenarios  $\mathcal{X}$ ; training episodes  $E$ ; the number of neighbor  $n$ ; the Upper Transformer input length  $K$ ;

**Initialize:** buffer  $\mathcal{D}$ ; parameters  $\theta$ ;

**Output:** Optimized policy  $\pi^\theta$

```
1: for episode=1, ..., E do
2:   clean buffer  $\mathcal{D} \leftarrow \emptyset$ ;
3:   for each scenario  $x \in \mathcal{X}$  do
4:     Find nearest  $n$  neighbors  $\mathcal{N}$  of each intersection;
5:     for each time step  $t$  do
6:       Get the last  $K$  transitions  $\{\mathbf{m}_{t-k+1}^i\}_{k=1, \dots, K}^x$  of
           each intersection  $i$  according to Eq. (1) and add
           these into  $\mathcal{D}$ ;
7:       Get action  $\mathbf{a}_t^i$  according to Eq. (9) and take joint
           action  $\{\mathbf{a}_t^1, \dots, \mathbf{a}_t^{n_x}\}$ ;
8:       Get the next states  $\mathbf{o}_{t+1}^i$ , and rewards  $\mathbf{r}_t^i$ ;
9:     end for
10:  end for
11:  for each step in training steps do
12:    sample minibatch data from  $\mathcal{D}$ ;
13:    Get dynamic predictions  $\{\hat{\mathbf{z}}_{t-k+1, i}^{\text{output}}\}_{k=1, \dots, K-1}$  ac-
           cording to Eq.(7);
14:    Compute  $\mathcal{L}$  according (10) and update parameter  $\theta$ ;
15:  end for
16: end for
```

---

from GESA [Jiang *et al.*, 2024], whose core idea is to map all various-structured intersections into a unified 4-leg one. This encourages the agent to learn generalist knowledge and also enables a more stable training process.

Lastly, the learning algorithm is shown in Algorithm 1.

## 4 Experiments

### 4.1 Datasets

We conducted experiments on the simulation of urban mobility (SUMO)<sup>1</sup> as the simulator. The duration of each episode is 3600 seconds. Seven different scenarios [Ault and Sharon, 2021; Jiang *et al.*, 2024] are employed in our co-training: five of them are reported in results, and another two scenarios (*Fenglin* and *Nanshan*) are only employed to increase the number of meta-training scenarios. To enable multi-scenario co-training, we utilize the GPI module in GESA to significantly reduce the need for manual labeling and unify the observation space and action space of all intersections. The main idea of GPI is to map all variously structured intersections into a unified 4-leg one using the relative angle and masking. For details, please refer to [Jiang *et al.*, 2024]. Table 1 shows the properties of different scenarios. The details about these scenarios are in Appx. D.

### 4.2 Baselines

To comprehensively verify the effectiveness of our proposed method, we employed four types of methods for a comprehensive comparison: Conventional methods, Multi-agent

Scenarios	Country	Type	#Total Int.	Scenarios	Country	Type	#Total Int.
<i>Grid</i> 4 × 4	synthetic	region	16	<i>Cologne8</i>	Germany	region	8
<i>Avenue</i> 4 × 4	synthetic	region	16	<i>Ingolstadt21</i>	Germany	region	12
<i>Grid</i> 5 × 5	synthetic	region	25	<i>Fenglin</i>	China	corridor	7
				<i>Nanshan</i>	China	region	28

Table 1: Statistics of the scenarios.

methods, Meta-Learning methods, and a combination of both Meta-Learning and Multi-agent methods.

#### Conventional methods:

- **Fixed Time Control (FTC)** [Roess *et al.*, 2004] with random offset executes each phase within a loop, utilizing a pre-defined phase duration.
- **MaxPressure** [Kouvelas *et al.*, 2014] is a powerful conventional method that consistently selects the phase with the highest pressure among all phases.

#### Multi-agent methods:

- **MPLight** [Chen *et al.*, 2020] is based on a phase competition mechanism to select which phase to execute, and utilizes the concept of pressure as state and reward to coordinate multiple intersections.
- **IPPO** [Ault and Sharon, 2021] controls each intersection with an independent PPO agent, and the agents at each intersection have the same model architecture but different model parameters.
- **rMAPPO** [Yu *et al.*, 2022a] is executed with independent PPO agents like IPPO, but it uses the overall information of all intersections to jointly optimize traffic efficiency. Furthermore, we use RNNs to introduce historical information into the agent.
- **CoLight** [Wei *et al.*, 2019b] utilizes the GAT to aggregate information from neighboring intersections, enhancing cooperation between intersections.

#### Meta-Learning and Single-agent methods:

- **MetaLight** [Zang *et al.*, 2020] using the meta-learning method to train multiple scenarios to increase the generalization of the model.
- **GESA** [Jiang *et al.*, 2024] proposes a unified state and action space, and subsequently employs the GPI module for large-scale multi-scenario collaborative training, which improves performance and generality.

#### Meta-Learning and Multi-agent methods:

- **MetaGAT** [Lou *et al.*, 2022] combines contextual meta-learning based on GRU to improve generalization and GAT for cooperation. Yet, the GRU is not scenario-agnostic trained, and GAT only uses observations  $o$ .
- **X-Light** (ours) and **X-Light<sub>GNN</sub>**, which replaces the Lower Transformer with GNN [Hamilton *et al.*, 2017], and the node feature of each intersection is obtained by concatenating  $o, a, r$  into a three times longer embedding, discarding the interrelations among them.

### 4.3 Evaluation Metrics

As same as most existing works [Lou *et al.*, 2022; Oroojlooy *et al.*, 2020; Chen *et al.*, 2020], we use **average trip time** as a

<sup>1</sup><https://www.eclipse.org/sumo/>

Methods	Avg. Trip Time (seconds)					Avg. Delay Time (seconds)				
	transfer to Grid4×4	transfer to Grid5×5	transfer to Arterial4×4	transfer to Ingolstadt21	transfer to Cologne8	transfer to Grid4×4	transfer to Grid5×5	transfer to Arterial4×4	transfer to Ingolstadt21	transfer to Cologne8
FTC	206.68 ± 0.54	550.38 ± 8.31	828.38 ± 8.17	319.41 ± 24.48	124.4 ± 1.99	94.64 ± 0.43	790.18 ± 7.96	1234.30 ± 6.50	183.70 ± 26.21	62.38 ± 2.95
MP	175.97 ± 0.70	274.15 ± 15.23	686.12 ± 9.57	375.25 ± 2.40	95.96 ± 1.11	64.01 ± 0.71	240.00 ± 18.43	952.53 ± 12.48	275.36 ± 14.38	31.93 ± 1.07
MetaLight	169.21 ± 1.16	<u>244.99 ± 8.18</u>	392.34 ± 4.39	298.67 ± 5.09	92.38 ± 0.94	57.82 ± 0.67	202.32 ± 11.20	850.42 ± 36.35	<u>166.35 ± 5.53</u>	28.37 ± 0.73
GESA	166.23 ± 1.07	284.05 ± 25.36	410.59 ± 2.60	318.30 ± 9.56	<u>88.76 ± 0.46</u>	54.69 ± 0.81	246.96 ± 37.62	972.87 ± 114.04	208.41 ± 12.01	<u>25.13 ± 0.64</u>
MetaGAT	165.18 ± 0.00	278.67 ± 0.00	379.47 ± 0.00	<u>288.10 ± 0.00</u>	90.41 ± 0.00	52.71 ± 0.00	241.51 ± 0.00	<u>753.88 ± 0.00</u>	177.10 ± 0.00	26.59 ± 0.00
Ours <sub>GNN</sub>	<u>164.46 ± 0.00</u>	249.64 ± 0.00	<u>366.97 ± 0.00</u>	298.97 ± 0.00	91.02 ± 0.00	<u>52.43 ± 0.00</u>	<u>194.36 ± 0.00</u>	762.61 ± 0.00	178.69 ± 0.00	27.26 ± 0.00
Ours	<b>162.65 ± 0.00</b> (+1.5%)	<b>243.26 ± 6.49</b> (+12.9%)	<b>361.38 ± 0.00</b> (+5.1%)	<b>280.20 ± 0.00</b> (+2.7%)	<b>88.49 ± 0.00</b> (+2.1%)	<b>50.90 ± 0.89</b> (+3.4%)	<b>193.84 ± 0.00</b> (+19.7%)	<b>705.48 ± 0.00</b> (+6.4%)	<b>160.42 ± 0.00</b> (+9.6%)	<b>24.71 ± 0.00</b> (+7.1%)

Table 2: Performance when transferring to an unseen scenario, with the format as “mean ± standard deviation (gain in % compared with the best baseline)”, the best **boldfaced** and second best underlined. We employ zero-shot transfer for evaluation: for each test scenario, we employ six other scenarios during the training process and then directly evaluate them in the respective test scenario. Our proposed method achieves the best performance in zero-shot transfer. (Some standard deviation = 0.00 because only two digits are kept.)

Methods	Avg. Trip Time (seconds)					Avg. Delay Time (seconds)				
	Grid4×4 (seen)	Grid5×5 (seen)	Arterial4×4 (seen)	Ingolstadt21 (seen)	Cologne8 (seen)	Grid4×4 (seen)	Grid5×5 (seen)	Arterial4×4 (seen)	Ingolstadt21 (seen)	Cologne8 (seen)
FTC	206.68 ± 0.54	550.38 ± 8.31	828.38 ± 8.17	319.41 ± 24.48	124.4 ± 1.99	94.64 ± 0.43	790.18 ± 7.96	1234.30 ± 6.50	183.70 ± 26.21	62.38 ± 2.95
MaxPressure	175.97 ± 0.70	274.15 ± 15.23	686.12 ± 9.57	375.25 ± 2.40	95.96 ± 1.11	64.01 ± 0.71	240.00 ± 18.43	952.53 ± 12.48	275.36 ± 14.38	31.93 ± 1.07
MPLight	179.51 ± 0.95	261.76 ± 6.60	541.29 ± 45.24	319.28 ± 10.48	98.44 ± 0.62	67.52 ± 0.97	213.78 ± 14.44	1083.18 ± 63.38	185.04 ± 10.70	34.38 ± 0.63
IPPO	167.62 ± 2.42	259.28 ± 9.55	431.31 ± 28.55	379.22 ± 34.03	90.87 ± 0.40	56.38 ± 1.46	243.58 ± 9.29	914.58 ± 36.90	247.68 ± 35.33	26.82 ± 0.43
rMAPPO	164.96 ± 1.87	300.90 ± 8.31	565.67 ± 44.8	453.61 ± 29.66	97.68 ± 2.03	53.65 ± 1.00	346.78 ± 28.25	1185.2 ± 167.48	372.2 ± 39.85	33.37 ± 1.97
CoLight	163.52 ± 0.00	242.37 ± 0.00	409.93 ± 0.00	337.46 ± 0.00	89.72 ± 0.00	51.58 ± 0.00	248.32 ± 0.00	776.61 ± 0.00	226.06 ± 0.00	25.56 ± 0.00
MetaLight	169.21 ± 1.16	247.83 ± 5.99	381.77 ± 12.85	292.26 ± 4.40	91.57 ± 0.75	57.56 ± 0.76	209.13 ± 19.40	862.32 ± 39.01	<u>164.80 ± 3.75</u>	27.61 ± 0.78
GESA	<b>161.33 ± 1.34</b>	252.11 ± 9.94	393.57 ± 13.72	320.02 ± 5.57	90.59 ± 0.74	<b>49.60 ± 0.71</b>	210.74 ± 13.56	775.22 ± 8.63	209.57 ± 3.32	26.50 ± 0.87
MetaGAT	165.23 ± 0.00	266.60 ± 0.00	<u>374.80 ± 0.87</u>	<u>290.73 ± 0.45</u>	90.74 ± 0.00	53.20 ± 0.00	234.80 ± 0.00	772.36 ± 0.00	176.86 ± 2.37	26.85 ± 0.00
Ours <sub>GNN</sub>	164.32 ± 0.00	<u>233.12 ± 0.00</u>	382.38 ± 0.00	319.98 ± 0.00	<u>89.29 ± 0.00</u>	51.83 ± 0.00	<u>204.24 ± 0.00</u>	<u>710.68 ± 0.00</u>	184.10 ± 0.00	<u>25.00 ± 0.00</u>
Ours	<u>162.47 ± 0.00</u> (-0.7%)	<b>220.63 ± 0.00</b> (+9.0%)	<b>349.60 ± 0.00</b> (+6.7%)	<b>278.05 ± 0.00</b> (+4.4%)	<b>88.55 ± 0.00</b> (+1.4%)	<b>50.27 ± 0.00</b> (-1.3%)	<b>187.74 ± 0.00</b> (+11.0%)	<b>697.79 ± 0.00</b> (+9.7%)	<b>160.39 ± 0.00</b> (+2.7%)	<b>24.31 ± 0.00</b> (+4.9%)

Table 3: Performance on various scenarios that is seen in the training: methods from FTC to CoLight are trained and tested on the same scenario of each column, and methods from MetaLight to Ours are trained with all seven scenarios, five of them have results in each column.

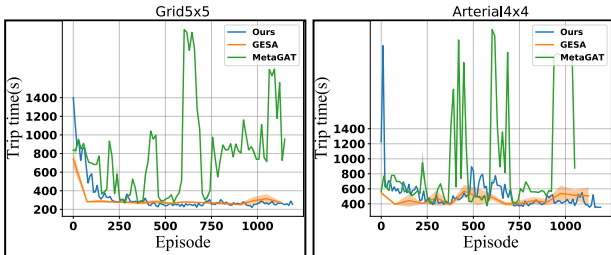


Figure 3: Trip time during the training process of Top 3 methods.

component of evaluation metrics, defined as the average time for each vehicle from entering the scenario to leaving the scenario. However, merely using the average trip time cannot accurately reflect the real traffic situation, e.g., in the cases of severe traffic congestion, new vehicles are prevented from entering the scenario, which leads to a relatively low average trip time though it is a severe traffic condition. Thus, we also add **average delay time** [Ault and Sharon, 2021] for evaluation, defined as the delay caused by signalized intersections and traffic congestion.

#### 4.4 Results

In this section, we show our proposed model’s superior transferability and general great performance.

##### Great Transferability When Handling A New Scenario

We use a zero-shot way to evaluate each model’s performance in transferring to new scenarios. Only transferable models are selected. In Table 2, each column means that we use the other six scenarios during training and then directly transfer to this unseen scenario. Our model achieves the best transfer results in all scenarios. (1) **Cooperation is needed:** Compared with single agent methods, e.g., MetaLight, cooperation is needed for better transferability. (2) **TonT is better for**

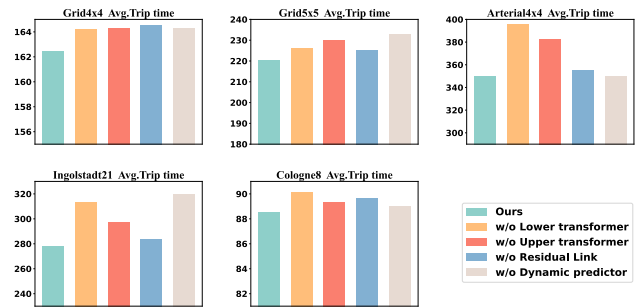


Figure 4: Ablation of each component in X-Light. The final solution attained the shortest trip time among all ablation experiments, showcasing the effectiveness of our design components.

**Meta MARL:** compared to the second-best MetaGAT, ours achieved a **+7.91%** improvement on average and **+16.3%** in *Grid5×5*, mainly because our unified Transformer on Transformer design captures collaborators’ *o*, *a*, *r* interdependency for better local cooperation, and global cross-scenario dynamics through multi-scenario co-training, respectively. Yet, MetaGAT only focuses on the neighbors’ *o* interdependency and lacks a scenario-agnostic training scheme. *In some cases (Grid5×5, Ingolstadt21), MetaGAT cannot beat MetaLight, which means that when cooperation is not as well designed as ours, it can even worsen the transferability when dealing with multi-scenarios.* (3) **Lower Transformer is better for cooperation:** ours<sub>GNN</sub> flattens *o*, *a*, *r*, thus losing the *o*, *a*, *r* interdependency, further highlighting the necessity of the Lower Transformer.

##### Enhanced Performance in Non-transfer Setting

In this non-transfer setting, as shown in Table 3, the scenario in each column is present in training: specifically, all meta-

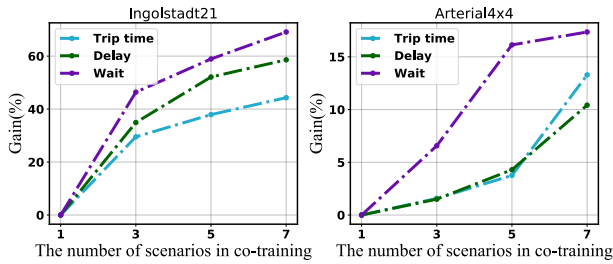


Figure 5: Impact of the number of scenarios co-training. As the number of scenarios increases, our performance also increases.

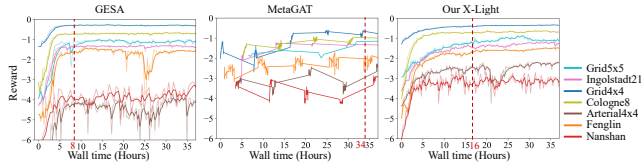


Figure 6: Training curve with wall times of the Top 3 methods. They utilize multi-scenarios during training. The red dotted line approximates convergence time.

learning-based methods from MetaLight to Ours are trained with all seven scenarios, while other methods from FTC to CoLight are trained and tested on the same one scenario. Figure 3 further plots the top three methods’ training process. (1) **TonT is also advantageous for non-transfer:** our method achieves the best results in four scenarios, with a **+6.20%** gain on average and **+9.96%** in *Grid5×5*. The gain is relatively lower than the Transfer setting, which is reasonable given we are dedicated to transfer. Besides, we have tiny **-1.02%** loss compared with the best GESA in the *Grid4×4*. A potential reason is the over-simplicity of the scenario. (2) **Our multi-scenario co-training is more stable than MetaGAT:** As shown in Figure 3, our training is much more stable than MetaGAT (both are multi-agent setting), due to the co-training design and strong scenario-agnostic trained Upper Transformer. GESA is the most stable given it is single-agent and also in a multi-scenario co-training scheme like ours.

### Better Convergence of X-Light

All the methods are trained for 37 hours and converged. In Fig. 6, we show the Training curve with wall times of the Top 3 methods. While GESA only takes 8 hours to converge, it shows inferior performance after convergence because it is single-agent RL. In multi-agent RL, our X-Light is around twice as fast as MetaGAT (16 hours over 34 hours); this is because GNN is computationally heavy. Furthermore, our Multi-scenario Co-Training, where intersections are stochastically chosen from various scenarios within each batch, has also contributed to more stable and beautiful training curves than MetaGAT.

### Ablation Studies

We conduct ablations to verify the necessity of the Lower and Upper Transformers, residual link, and dynamic predictor.

- **w/o Lower Transformer** replaces the Lower Transformer with MLP. No collaboration is formulated.

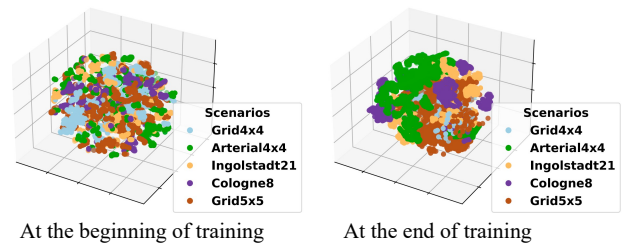


Figure 7: Visualizing Upper Transformer’s output  $\mathbf{z}^{\text{output}}$ . Our model can group the decision dynamics from the same scenario together.

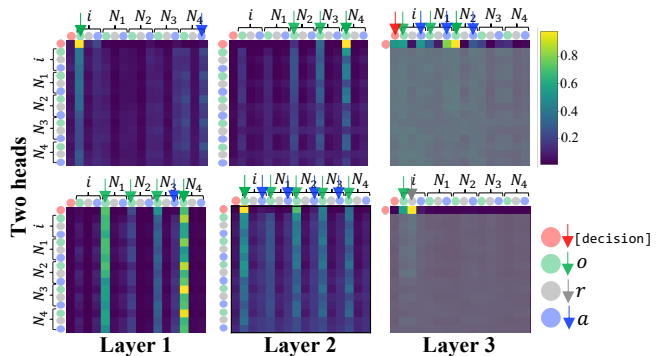


Figure 8: Visualizing Lower Transformer’s attention (*Cologne8*), with top attentions marked with  $\downarrow$ . Each row in attention is the weight of the corresponding token w.r.t all other tokens. We pick 2 heads over 3 layers. The last layer exclusively uses the [decision] token (only the first row is shown). Lower Transformer efficiently models these MDP features’ interrelations: more attention to  $o$  in shallow layers, and more to  $a, r$  in deeper layers.

- **w/o Upper Transformer** replaces the Upper Transformer with GRU.
- **w/o Residual Link** removes the  $\mathbf{o}_i^t$  in the actor input.
- **w/o Dynamic predictor** removes the dynamic predictor in the Upper Transformer, thus without  $\mathcal{L}_{pred}$ .

Figure 4 shows the trip time results, with other metrics in Appx. F. We can conclude that (1) the Lower Transformer, which promotes collaboration, is the most critical component. (2) In the Upper Transformer, the Transformer model is better than GRU; moreover, the dynamic predictor is also very necessary to ensure the Upper Transformer learns scenario-diagnostic dynamics. (3) As discussed before, the residual link can further boost performance, especially in easier scenarios such as *Grid4×4* and *Cologne8*, where the direct self-observation is more useful for decision in simple scenarios.

**Numbers of co-trained scenarios:** in Figure 5, we also conducted the impact of different numbers of co-training scenarios. We increase the number of co-trained scenarios from 1 to 7 and test in the two fixed scenarios (*Ingolstadt21* and *Arterial4×4*). Our method consistently improves as the number of co-training scenarios increases.

We also conducted experiments on the Upper Transformer, exploring various historical lengths, with details in Appx. F.

### Visualizing X-Light’s Upper and Lower Transformers

This visualization offers great insights on our TonT.

**Upper Transformer understands the scenario dynamics well:** We first analyze the output embeddings from the Upper Transformer. In Figure 7, we visualize the model before and after training in five evaluation scenarios with the 3D t-SNE technique, and each scenario has a unique color. The Upper Transformer can map dynamics from the same scenario together, demonstrating the Upper Transformer’s good understanding of various scenario dynamics.

**Lower Transformer collaborates well by fully utilizing  $o, a, r$ :** Furthermore, we visualize the attention weights of the Lower Transformers. In Figure 8, we visualize attention weights for two heads across three layers in the *Cologne8*. We find that (1) in the shallow Layer-1, attention is mainly to observations (green) of the target and its neighbors via different heads; in deeper Layer-2, more attention is to actions (blue); in deepest Layer-3, right the output being used for decision, all  $o, r, a$ , especially rewards (grey), have high attention (more cases in Appx. G); (2) This further justify the necessity of our Lower Transformer, with superiority of modeling  $o, r, a$ -interrelation over GNN-based collaborations.

## 5 Discussions

In this section, we will discuss a few key questions the audience may be interested in.

**Discussion on Scalability:** Our model is scalable since it’s decentralized: when it takes action, it only requires self-observation and observations of the nearest neighbor intersections. In reality, when controlling the traffic signals of a whole city, commonly the city is partitioned into multiple subareas according to the intersections’ similarities in structure and traffic conditions [Guo *et al.*, 2014], with a subarea usually 4-7 intersections spatial spanning within 1 kilometer. This subarea control strategy is more effective and flexible when the traffic conditions differ between different districts.

**Discussion on compatibility of X-Light towards constraints on stages and cycle lengths:** Can our X-Light consider existing constraints on stages and cycle lengths, and deal with min-max green durations and pedestrian crossings? The answer is positive: our transformer-on-transformer (TonT) from X-Light is a general framework for transferring across cities; as long as the backbone RL-based TSC model considers the constraints, X-Light can also do it. In this work, we use FRAP as the RL backbone, which is an acyclic action that does not have a “cycle” of phases. When applying our method for cyclic control, we can change our backbone RL model to [Liang *et al.*, 2019] (e.g., action is to +/- 5 seconds on a phase, or remain the same) and add maximum/minimum green durations or cycle length constraints (e.g., disable the action of +5s if when exceeding max-duration).

**Discussion on transfer assumption for different regions** We will discuss from the two perspectives of junction and phase. **Junction-wise:** No specific requirements on the number of legs/movements: Since we use the GPI module, it maps various junctions into a unified structure, e.g., non-existing movements’ states and actions will be zero-padded. **n Phase-wise:** Since we are acyclic control, we only need the common setting: each selected phase runs for 10s, and the yellow light is 3s.

**Discussion on the potential guarantees of the generated strategies** Firstly, the evaluation methodology of our zero-shot experiments validates the policies’ generalization capabilities. Secondly, theoretical guarantees on performance lower bounds can be assured. The performance in unseen scenarios can be proven to exceed a polynomial function of the tasks’ maximum mean discrepancy. The proof follows [Rostami *et al.*, 2020].

## 6 Conclusion

In this paper, we propose X-Light, an innovative framework that has two types of transformers with multi-scenario co-training. This design enhances the agent’s transferability and enables collaboration across multiple intersections simultaneously. We use a large number of scenarios and comparison methods to verify the effectiveness of our proposed method. The outcomes highlight not only the exceptional performance of our method but also its robust transferability.

For future work, we aim to transition our methodology into real-world applications, addressing the challenging sim2real problem. We hold the belief that this endeavor will significantly enhance urban traffic efficiency.

## References

- [Arnab *et al.*, 2021] Anurag Arnab, Mostafa Dehghani, Georg Heigold, Chen Sun, Mario Lučić, and Cordelia Schmid. Vivit: A video vision transformer. In *2021 IEEE/CVF International Conference on Computer Vision (ICCV)*, pages 6816–6826, 2021.
- [Ault and Sharon, 2021] James Ault and Guni Sharon. Reinforcement learning benchmarks for traffic signal control. In *Thirty-fifth Conference on Neural Information Processing Systems Datasets and Benchmarks Track (Round 1)*, 2021.
- [Chen *et al.*, 2020] Chacha Chen, Hua Wei, Nan Xu, Guanjie Zheng, Ming Yang, Yuanhao Xiong, Kai Xu, and Zhenhui Li. Toward a thousand lights: Decentralized deep reinforcement learning for large-scale traffic signal control. In *Proceedings of the AAAI Conference on Artificial Intelligence*, volume 34, pages 3414–3421, 2020.
- [Chen *et al.*, 2021] Lili Chen, Kevin Lu, Aravind Rajeswaran, Kimin Lee, Aditya Grover, Misha Laskin, Pieter Abbeel, Aravind Srinivas, and Igor Mordatch. Decision transformer: Reinforcement learning via sequence modeling. *Advances in neural information processing systems*, 34:15084–15097, 2021.
- [Chu *et al.*, 2019] Tianshu Chu, Jie Wang, Lara Codecà, and Zhaojian Li. Multi-agent deep reinforcement learning for large-scale traffic signal control. *IEEE Transactions on Intelligent Transportation Systems*, 21(3):1086–1095, 2019.
- [Dosovitskiy *et al.*, 2020] Alexey Dosovitskiy, Lucas Beyer, Alexander Kolesnikov, Dirk Weissenborn, Xiaohua Zhai, Thomas Unterthiner, Mostafa Dehghani, Matthias Minderer, Georg Heigold, Sylvain Gelly, et al. An image is worth 16x16 words: Transformers for image recognition at scale. *arXiv preprint arXiv:2010.11929*, 2020.



- [Du *et al.*, 2024] Xinqi Du, Ziyue Li, Cheng Long, Yongheng Xing, S Yu Philip, and Hechang Chen. Felight: Fairness-aware traffic signal control via sample-efficient reinforcement learning. *IEEE Transactions on Knowledge and Data Engineering*, 2024.
- [Duan *et al.*, 2017] Yan Duan, John Schulman, Xi Chen, Peter L. Bartlett, Ilya Sutskever, and Pieter Abbeel. RL<sup>2</sup>: Fast reinforcement learning via slow reinforcement learning, 2017.
- [El-Tantawy *et al.*, 2013] Samah El-Tantawy, Baher Abdulhai, and Hossam Abdelgawad. Multiagent reinforcement learning for integrated network of adaptive traffic signal controllers (MARLIN-ATSC): Methodology and large-scale application on downtown Toronto. *IEEE Transactions on Intelligent Transportation Systems*, 14(3):1140–1150, 2013.
- [Goodfellow *et al.*, 2014] Ian Goodfellow, Jean Pouget-Abadie, Mehdi Mirza, Bing Xu, David Warde-Farley, Sherjil Ozair, Aaron Courville, and Yoshua Bengio. Generative adversarial nets. *Advances in neural information processing systems*, 27, 2014.
- [Guo *et al.*, 2014] Haifeng Guo, Jun Cheng, Qitao Peng, Chao Zhu, and Yuanjie Mu. Dynamic division of traffic control sub-area methods based on the similarity of adjacent intersections. In *17th International IEEE Conference on Intelligent Transportation Systems (ITSC)*, pages 2208–2213. IEEE, 2014.
- [Guo *et al.*, 2021] Xin Guo, Zhengxu Yu, Pengfei Wang, Zhongming Jin, Jianqiang Huang, Deng Cai, Xiaofei He, and Xiansheng Hua. Urban traffic light control via active multi-agent communication and supply-demand modeling. *IEEE Transactions on Knowledge and Data Engineering*, 2021.
- [Hamilton *et al.*, 2017] Will Hamilton, Zhitao Ying, and Jure Leskovec. Inductive representation learning on large graphs. *Advances in neural information processing systems*, 30, 2017.
- [Han *et al.*, 2021] Kai Han, An Xiao, Enhua Wu, Jianyuan Guo, Chunjing Xu, and Yunhe Wang. Transformer in transformer. *Advances in Neural Information Processing Systems*, 34:15908–15919, 2021.
- [Humphrik *et al.*, 2019] Jan Humphrik, Alexandre Galashov, Leonard Hasenclever, Pedro A Ortega, Yee Whye Teh, and Nicolas Heess. Meta reinforcement learning as task inference. *arXiv preprint arXiv:1905.06424*, 2019.
- [Hunt *et al.*, 1982] PB Hunt, DI Robertson, RD Bretherton, and M Cr Royle. The SCOOT on-line traffic signal optimisation technique. *Traffic Engineering & Control*, 23(4), 1982.
- [Janner *et al.*, 2021] Michael Janner, Qiyang Li, and Sergey Levine. Offline reinforcement learning as one big sequence modeling problem. *Advances in neural information processing systems*, 34:1273–1286, 2021.
- [Jiang *et al.*, 2024] Haoyuan Jiang, Ziyue Li, Zhishuai Li, Lei Bai, Hangyu Mao, Wolfgang Ketter, and Rui Zhao. A general scenario-agnostic reinforcement learning for traffic signal control. *IEEE Transactions on Intelligent Transportation Systems*, 2024.
- [Kouvelas *et al.*, 2014] Anastasios Kouvelas, Jennie Lioris, S Alireza Fayazi, and Pravin Varaiya. Maximum pressure controller for stabilizing queues in signalized arterial networks. *Transportation Research Record*, 2421(1):133–141, 2014.
- [Liang *et al.*, 2019] Xiaoyuan Liang, Xunsheng Du, Guiling Wang, and Zhu Han. A deep reinforcement learning network for traffic light cycle control. *IEEE Transactions on Vehicular Technology*, 68(2):1243–1253, 2019.
- [Liang *et al.*, 2022] Yuxuan Liang, Pan Zhou, Roger Zimmermann, and Shuicheng Yan. Dualformer: Local-global stratified transformer for efficient video recognition. In Shai Avidan, Gabriel Brostow, Moustapha Cissé, Giovanni Maria Farinella, and Tal Hassner, editors, *Computer Vision – ECCV 2022*, pages 577–595, Cham, 2022. Springer Nature Switzerland.
- [Lou *et al.*, 2022] Yican Lou, Jia Wu, and Yunchuan Ran. Meta-reinforcement learning for multiple traffic signals control. In *Proceedings of the 31st ACM International Conference on Information & Knowledge Management*, pages 4264–4268, 2022.
- [Lowrie, 1990] PR Lowrie. SCATS, Sydney co-ordinated adaptive traffic system: A traffic responsive method of controlling urban traffic. 1990.
- [Lu *et al.*, 2023] Jiaming Lu, Jingqing Ruan, Haoyuan Jiang, Ziyue Li, Hangyu Mao, and Rui Zhao. Dualight: Enhancing traffic signal control by leveraging scenario-specific and scenario-shared knowledge. *arXiv preprint arXiv:2312.14532*, 2023.
- [Mao *et al.*, 2023] Hangyu Mao, Rui Zhao, Ziyue Li, Zhiwei Xu, Hao Chen, Yiqun Chen, Bin Zhang, Zhen Xiao, Junge Zhang, and Jiangjin Yin. Pdit: Interleaving perception and decision-making transformers for deep reinforcement learning. *arXiv preprint arXiv:2312.15863*, 2023.
- [Melo, 2022] Luckeciano C Melo. Transformers are meta-reinforcement learners. In *international conference on machine learning*, pages 15340–15359. PMLR, 2022.
- [Nishi *et al.*, 2018] Tomoki Nishi, Keisuke Otaki, Keiichiro Hayakawa, and Takayoshi Yoshimura. Traffic signal control based on reinforcement learning with graph convolutional neural nets. In *2018 21st International conference on intelligent transportation systems (ITSC)*, pages 877–883. IEEE, 2018.
- [Oroojlooy *et al.*, 2020] Afshin Oroojlooy, Mohammadreza Nazari, Davood Hajinezhad, and Jorge Silva. Attendlight: Universal attention-based reinforcement learning model for traffic signal control. *Advances in Neural Information Processing Systems*, 33:4079–4090, 2020.
- [Prashanth and Bhatnagar, 2010] LA Prashanth and Shalabh Bhatnagar. Reinforcement learning with function approximation for traffic signal control. *IEEE Transactions on Intelligent Transportation Systems*, 12(2):412–421, 2010.

- [Prashanth and Bhatnagar, 2011] LA Prashanth and Shalabh Bhatnagar. Reinforcement learning with average cost for adaptive control of traffic lights at intersections. In *2011 14th International IEEE Conference on Intelligent Transportation Systems (ITSC)*, pages 1640–1645. IEEE, 2011.
- [Roess *et al.*, 2004] Roger P Roess, Elena S Prassas, and William R McShane. *Traffic engineering*. Pearson/Prentice Hall, 2004.
- [Rostami *et al.*, 2020] Mohammad Rostami, David Isele, and Eric Eaton. Using task descriptions in lifelong machine learning for improved performance and zero-shot transfer. *Journal of Artificial Intelligence Research*, 67:673–704, 2020.
- [Schulman *et al.*, 2017] John Schulman, Filip Wolski, Prafulla Dhariwal, Alec Radford, and Oleg Klimov. Proximal policy optimization algorithms. *arXiv preprint arXiv:1707.06347*, 2017.
- [Van der Pol and Oliehoek, 2016] Elise Van der Pol and Frans A Oliehoek. Coordinated deep reinforcement learners for traffic light control. *Proceedings of Learning, Inference and Control of Multi-agent Systems (at NIPS 2016)*, 1, 2016.
- [Vaswani *et al.*, 2017] Ashish Vaswani, Noam Shazeer, Niki Parmar, Jakob Uszkoreit, Llion Jones, Aidan N Gomez, Łukasz Kaiser, and Illia Polosukhin. Attention is all you need. *Advances in neural information processing systems*, 30, 2017.
- [Wei *et al.*, 2019a] Hua Wei, Chacha Chen, Guanjie Zheng, Kan Wu, Vikash Gayah, Kai Xu, and Zhenhui Li. Presslight: Learning max pressure control to coordinate traffic signals in arterial network. In *Proceedings of the 25th ACM SIGKDD International Conference on Knowledge Discovery & Data Mining*, pages 1290–1298, 2019.
- [Wei *et al.*, 2019b] Hua Wei, Nan Xu, Huichu Zhang, Guanjie Zheng, Xinshi Zang, Chacha Chen, Weinan Zhang, Yanmin Zhu, Kai Xu, and Zhenhui Li. Colight: Learning network-level cooperation for traffic signal control. In *Proceedings of the 28th ACM International Conference on Information and Knowledge Management*, pages 1913–1922, 2019.
- [Wei *et al.*, 2021] Hua Wei, Guanjie Zheng, Vikash Gayah, and Zhenhui Li. Recent advances in reinforcement learning for traffic signal control: A survey of models and evaluation. *ACM SIGKDD Explorations Newsletter*, 22(2):12–18, 2021.
- [Wolshon *et al.*, 2016] Brian Wolshon, Anurag Pande, et al. *Traffic engineering handbook*. John Wiley & Sons, 2016.
- [Wu *et al.*, 2023] Qiang Wu, Mingyuan Li, Jun Shen, Linyuan Lü, Bo Du, and Ke Zhang. Transformerlight: A novel sequence modeling based traffic signaling mechanism via gated transformer. In *Proceedings of the 29th ACM SIGKDD Conference on Knowledge Discovery and Data Mining*, KDD '23, page 2639–2647, New York, NY, USA, 2023. Association for Computing Machinery.
- [Xu *et al.*, 2013] Lun-Hui Xu, Xin-Hai Xia, and Qiang Luo. The study of reinforcement learning for traffic self-adaptive control under multiagent markov game environment. *Mathematical Problems in Engineering*, 2013, 2013.
- [Xu *et al.*, 2022] Mengdi Xu, Yikang Shen, Shun Zhang, Yuchen Lu, Ding Zhao, Joshua Tenenbaum, and Chuang Gan. Prompting decision transformer for few-shot policy generalization. In *international conference on machine learning*, pages 24631–24645. PMLR, 2022.
- [Yau *et al.*, 2017] Kok-Lim Alvin Yau, Junaid Qadir, Hooi Ling Khoo, Mee Hong Ling, and Peter Komisarczuk. A survey on reinforcement learning models and algorithms for traffic signal control. *ACM Computing Surveys (CSUR)*, 50(3):1–38, 2017.
- [Yu *et al.*, 2022a] Chao Yu, Akash Velu, Eugene Vinitzky, Jiaxuan Gao, Yu Wang, Alexandre Bayen, and Yi Wu. The surprising effectiveness of ppo in cooperative multi-agent games. *Advances in Neural Information Processing Systems*, 35:24611–24624, 2022.
- [Yu *et al.*, 2022b] Rui Yu, Dawei Du, Rodney LaLonde, Daniel Davila, Christopher Funk, Anthony Hoogs, and Brian Clipp. Cascade transformers for end-to-end person search. In *Proceedings of the IEEE/CVF Conference on Computer Vision and Pattern Recognition (CVPR)*, pages 7267–7276, June 2022.
- [Zang *et al.*, 2020] Xinshi Zang, Huaxiu Yao, Guanjie Zheng, Nan Xu, Kai Xu, and Zhenhui Li. Metalight: Value-based meta-reinforcement learning for traffic signal control. In *Proceedings of the AAAI Conference on Artificial Intelligence*, volume 34, pages 1153–1160, 2020.
- [Zhang *et al.*, 2020] Huichu Zhang, Chang Liu, Weinan Zhang, Guanjie Zheng, and Yong Yu. Generalight: Improving environment generalization of traffic signal control via meta reinforcement learning. In *Proceedings of the 29th ACM International Conference on Information & Knowledge Management*, pages 1783–1792, 2020.
- [Zheng *et al.*, 2019] Guanjie Zheng, Yuanhao Xiong, Xinshi Zang, Jie Feng, Hua Wei, Huichu Zhang, Yong Li, Kai Xu, and Zhenhui Li. Learning phase competition for traffic signal control. In *Proceedings of the 28th ACM International Conference on Information and Knowledge Management*, pages 1963–1972, 2019.
- [Zhu *et al.*, 2023] Liwen Zhu, Peixi Peng, Zongqing Lu, and Yonghong Tian. Metavim: Meta variationally intrinsic motivated reinforcement learning for decentralized traffic signal control. *IEEE Transactions on Knowledge and Data Engineering*, 2023.

# Appendices

In Appx. A, we will introduce the preliminary of this work. In Appx. B, we will present additional related work on multi-agent RL for TSC and applying two transformers in other fields. In Appx. C, we will provide details regarding the implementation details of X-Light. In Appx. D, we will present more detailed statistics about the scenarios. In Appx. E, we introduce a new metric to evaluate each method and also demonstrate that our proposed method still state-of-the-art. In Appx. F, we document additional results from the ablation studies. Lastly, in Appx. G, we present more visualization attention weights of the Lower Transformer.

## A Preliminary

### A.1 Definitions

In this paper, we investigate traffic signal control of multi-intersection with different scenarios. To explain the basic concepts, we use a sample scenario with 9 intersections, and each intersection is a 4-arm intersection as shown in Figure A1. The red box is the target intersection, the blue boxes indicate its neighbor intersections.

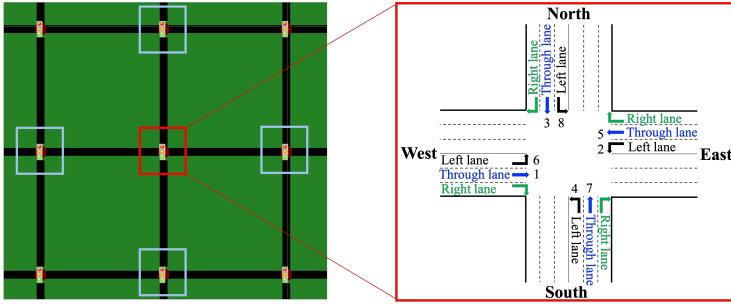


Figure A1: A simple scenario and a standard intersection structure. The red box is the target intersection and the blue box is its nearest top 4 neighbor intersections.

Phase	Movements
A	← + →
B	↖ + ←
C	→ + ↘
D	↖ + ↘
E	↓ + ↑
F	↙ + ↓
G	↓ + ↘
H	↙ + ↘

Figure A2: Enumerates eight typical signal phases

**Definition 1. Entering Lanes:** For each intersection, the entering lanes indicate that vehicles can enter the intersection from these lanes. On the right of Figure A1, a standard intersection has four approaches: north, east, south, and west, and each approach has three types of entering lanes: left lane, through lane, and right lane, therefore there are total 12 different movements for this intersection. In the real world, most intersections have four approaches, but some have 3-arm or 5-arm.

**Definition 2. Phase:** By selecting the execution phase of the next time step is a common way of traffic signal control. In the real world, we commonly do not control the left entering lanes [Wolshon *et al.*, 2016]. As shown in Figure A2, there are 8 typical signal phases in total, each of them consisting of two different and non-conflict movements. When a phase is executed, only the vehicles on the entering lanes of the phase can continue to drive.

### A.2 Problem Statement

We define the problem of multi-agent traffic signal control in different scenarios as Meta-RL partially observed Markov decision processes (Meta-RL POMDPs) [Humplik *et al.*, 2019]. Given a set of scenarios  $\mathcal{X}$  sampled over task distribution  $\varepsilon$ . Each agent controls one of the intersections  $I_i$  from a scenario  $x$ , and each intersection has its top  $n$  nearest neighboring intersections  $\mathbf{I}_{\mathcal{N}_i}$ , where  $\mathcal{N}_i = \{N_1, \dots, N_n\}$ . Each agent observes part of the total system condition which only includes the transition information of the target intersection  $i$  and its top  $n$  nearest neighbor intersections. We can represent this as  $\langle \mathcal{S}, \mathcal{O}, \mathcal{A}, \mathcal{P}, r, \gamma \rangle$ .  $\mathcal{S}$  is the state space, and  $s_t \in \mathcal{S}$  denotes the state at time step  $t$ . The observation is acquired through an observation function  $D(s) : \mathcal{S} \rightarrow \mathcal{O}$ .  $\mathcal{A}$  is the action space for each agent. At time step  $t$ , all agents in a scenario takes a joint action  $\mathbf{a}_t^{all} := \{\mathbf{a}_t^1, \dots, \mathbf{a}_t^{n_x}\}$ ,  $n_x$  is the total number of the scenario  $x$  and cause the state transition  $\mathcal{P}(s_{t+1}|s_t, \mathbf{a}_t^{all}) := \mathcal{S} \times \mathcal{A}^{n_x} \rightarrow \mathcal{S}$  and agent  $i$  received a reward  $r_t^i$ . Since the environment is partially observed, each agent only has access to its local observations, rewards and actions:  $o_t^{\{i, \mathcal{N}_i\}}$ ,  $a_{t-1}^{\{i, \mathcal{N}_i\}}$ , and  $r_{t-1}^{\{i, \mathcal{N}_i\}}$ . When optimizing, we want to maximize cumulative reward for each agent:  $\sum_t \gamma^t r_t^i$ , where  $\gamma$  is the discounted factor.

In meta-reinforcement learning, we need to be able to achieve great performance in a variety of scenarios, even if these scenarios have never been encountered before. As shown in Figure 1, different surfaces represent different tasks, one goal is to learn  $\theta$  to make a distinction among the tasks in the embedding space  $\theta$ , and minimize loss across different tasks:

$$\theta = \arg \min_{\theta} \frac{1}{m} \sum_{i=1}^m \mathcal{L}(f_{\theta}(I_i), I_i) \quad (11)$$

where  $\theta$  is the policy parameter;  $f_{\theta}(I_i)$  is the policy output, which denotes the policy to solve the task  $I_i$ ;  $\mathcal{L}$  is the loss.

## B More Related Work

### B.1 Multi-Agent RL for TSC

Multi-Agent RL-based TSC methods aim to optimize the efficiency of vehicle traffic within a given area by learning the collaboration among intersections. Early research in this area [Prashanth and Bhatnagar, 2011; Van der Pol and Oliehoek, 2016; Xu *et al.*, 2013; Prashanth and Bhatnagar, 2010] through centralized optimization over joint actions among all intersections of a scenario. But this will cause two problems: 1. As the number of intersections increases, there will be a problem of dimensionality curse. 2. This approach does not generalize in meeting new scenarios. To counter these issues, independent or decentralized methods are proposed. One way [Chen *et al.*, 2020] is to guide cooperation by introducing the Pressure in the state and reward, which can reflect the intersection state associated with the upstream and downstream. Another way [El-Tantawy *et al.*, 2013; Nishi *et al.*, 2018; Chu *et al.*, 2019; Wei *et al.*, 2019b; Guo *et al.*, 2021] is to include neighbor information into states or hidden states. Although they can all cooperate well with their neighbors, these methods are used in simple scenarios and the relationship between neighbors is static. For a new scenario, the state transitions between themselves and their neighbors are often quite different.

### B.2 Applying Two Transformers in Other Fields.

In computer vision, some methods apply two Transformers to handle tasks like image classification and person search, e.g., TNT [Han *et al.*, 2021], ViViT [Arnab *et al.*, 2021], DualFormer [Liang *et al.*, 2022] and COAT [Yu *et al.*, 2022b]. However, our TonT model and these works are totally different. For example, TNT’s outer Transformer takes the coarse-grain patches, and the inner one further takes the finer patches from the coarse patch. For our TonT, the lower Transformer is to perceive the environment dynamics and decides on collaboration: it reads the MDP including  $o, a, r$  and uses attention to aggregate that information from the target and neighbor, and the upper transformer is to make the scenario-agnostic decision: it learns through the various scenarios decision dynamic and gain generalizability via memory reinstatement mechanism. As a result, TNT can only be used for vision tasks, but our TonT is designed for RL-based TSC tasks.

## C Implementation details of X-Light

In this section, we will give implementation details of X-Light.

First, we will introduce how to get the state  $o_t^i$ . Initially, we utilize the GPI module proposed in GESA to reduce manual labeling and structured intersections with different lane counts and orientations. Subsequently, to obtain the state  $o_t^i$ , we concatenate each feature obtained from the MLPs. It can be formulated as below:

$$\begin{aligned}\tilde{o}_{t,b}^i &= GPI(o_{t,b}^i), \\ o_t^i &= \parallel_{b=1}^B Sigmoid(MLP_b(\tilde{o}_{t,b}^i))\end{aligned}\tag{12}$$

where  $B$  is the number of total state features, *Sigmoid* is the activation function, and  $\parallel$  denotes concatenation.

Furthermore, the training parameters and the weight of each reward component can be found in Table A1.

## D The Detailed statistics about the scenarios

The important attributes of the scenarios are shown in Table A2, including the total amount of intersections(Total Int.), the number of traffic flow types in each scenario(Flow type), and the amount of 2-arm to 4-arm intersections.

In actual traffic networks, numerous intersections deviate from the standard four-arm configuration, exhibiting varying numbers of lanes and orientations. To ensure the broad applicability of our approach across diverse scenarios, we deliberately conduct experiments within the contexts of two non-standard intersections: *Cologne8* and *Ingolstadt21*.

These scenarios include not only typical four-arm intersections but also irregular intersections where the number and orientations of lanes deviate from the standard. Through experiments conducted in such settings, we demonstrate that our method not only effectively handles standard intersections, but also excels in managing these irregularities. This further emphasizes the robustness and potential wide applicability of our method.

## E The main results on the evaluation metric of average waiting time

Beside, two metric used in the main paper. We further add **average wait time** to compare various methods. The average waiting time represents how long each car was stopped.

The performance of our method in terms of average waiting time for new scenarios(zero-shot transfer) is presented in the Table A3. It can be observed that in the metric of waiting time, our method also achieves the best results. The performance of various methods on average waiting time for non-transfer is shown in Table A4. The results are consistent with the conclusions of the main results on paper. Finally, considering all three metrics(Trip time, Delay time, and Wait time), our algorithm has improved by 8.11% compared with the best result in the baselines.

Items	Details
Learning rate	5e-4
Actor loss coefficient $\alpha$	1
Critic loss coefficient $\beta$	1
Dynamic predictor loss coefficient $\kappa$	1e-2
Entropy coefficient	1e-2
GAE $\lambda$	0.95
Discount factor $\gamma$	0.99
Clipping $\epsilon$	0.2
Number of Lower transformer layer	3
Number of Lower transformer head	6
Number of Upper transformer layer	3
Number of Upper transformer head	6
Lower transformer embedding dimension $d$	114
Upper transformer embedding dimension $d'$	114
Upper transformer horizon $K$	20
The number of neighbor intersections $n$	4
Weight of Queue length in Reward	-1e-3
Weight of Wait time in Reward	-1e-3
Weight of Delay time in Reward	-1e-5
Weight of Pressure in Reward	-5e-3

Table A1: Implementation details of X-Light

Scenarios	Country	Type	#Total Int.	#Flow types	#2-arm	#3-arm	#4-arm
<i>Grid 4 × 4</i>	synthetic	region	16	1400	0	0	16
<i>Avenue 4 × 4</i>	synthetic	region	16	1400	0	0	16
<i>Grid 5 × 5</i>	synthetic	region	25	2	0	0	25
<i>Cologne8</i>	Germany	region	8	1	1	3	4
<i>Ingolstadt21</i>	Germany	region	12	1	0	8	4
<i>Fenglin</i>	China	corridor	7	1	0	2	5
<i>Nanshan</i>	China	region	28	1	1	6	21

Table A2: Statistics of the scenarios

Methods	Avg. Wait Time (seconds)				
	<i>transfer to Grid4×4</i>	<i>transfer to Grid5×5</i>	<i>transfer to Arterial4×4</i>	<i>transfer to Ingolstadt21</i>	<i>transfer to Cologne8</i>
FTC	66.12 ± 0.32	408.25 ± 7.09	599.10 ± 6.40	127.31 ± 20.06	35.30 ± 1.05
MaxPressure	37.78 ± 0.65	116.85 ± 12.50	495.52 ± 10.52	184.97 ± 3.56	11.19 ± 0.44
MetaLight	31.73 ± 0.49	<u>106.36 ± 6.00</u>	212.63 ± 4.26	110.55 ± 5.03	8.52 ± 0.23
GESA	28.45 ± 0.72	135.22 ± 20.44	242.32 ± 2.72	135.07 ± 8.02	<u>7.14 ± 0.19</u>
MetaGAT	<u>26.46 ± 0.00</u>	120.72 ± 0.00	<u>208.18 ± 0.00</u>	<u>99.45 ± 0.00</u>	7.98 ± 0.00
Ours	<b>24.71 ± 0.00</b>	<b>97.67 ± 3.31</b>	<b>206.45 ± 0.00</b>	<b>94.17 ± 0.00</b>	<b>7.07 ± 0.00</b>

Table A3: Avg. wait time for transferring to unseen scenarios. The best **boldfaced** and second best underlined. Our method also achieves the best.

## F The detailed results of the ablation studies

In this section, we will the detailed results of the ablation studies, and all of these contain all three metrics.

Table A5 and Table A6 show the effect of increasing the number of co-training scenarios. we can see that as the number of co-training scenarios increases, the results of the three metrics and stability continue to improve. The increase in the number of scenarios enhances the diversity of data available to the model, thereby preventing the model from becoming trapped in a local optimum caused by data distribution bias [Jiang *et al.*, 2024].

Table A7 shows the impact of important components in our proposed model, we found that each of these key components

Methods	Avg. Wait Time (seconds)				
	<i>Grid4×4 (seen)</i>	<i>Grid5×5 (seen)</i>	<i>Arterial4×4 (seen)</i>	<i>Ingolstadt21 (seen)</i>	<i>Cologne8 (seen)</i>
FTC	66.12 ± 0.32	408.25 ± 7.09	599.10 ± 6.40	127.31 ± 20.06	35.30 ± 1.05
MaxPressure	37.78 ± 0.65	116.85 ± 12.50	495.52 ± 10.52	184.97 ± 3.56	11.19 ± 0.44
MPLight	41.14 ± 0.79	106.82 ± 4.26	349.69 ± 43.48	130.57 ± 9.31	12.06 ± 0.32
IPPO	29.59 ± 1.15	108.61 ± 8.75	289.89 ± 25.53	185.88 ± 32.55	8.47 ± 0.20
rMAPPO	27.07 ± 0.54	153.38 ± 7.44	407.25 ± 41.15	264.41 ± 28.36	14.01 ± 1.12
CoLight	25.56 ± 0.00	100.58 ± 0.00	247.88 ± 0.00	147.91 ± 0.00	8.18 ± 0.00
MetaLight	31.79 ± 0.71	<u>98.57 ± 5.32</u>	241.88 ± 11.29	104.08 ± 3.65	8.44 ± 0.31
GESA	<b>23.86 ± 0.58</b>	102.98 ± 8.66	234.78 ± 6.02	136.43 ± 5.47	<u>7.59 ± 0.28</u>
MetaGAT	27.25 ± 0.00	123.78 ± 0.00	<u>219.36 ± 0.27</u>	<u>103.35 ± 0.62</u>	8.18 ± 0.00
Ours	<u>24.57 ± 0.00</u>	<b>79.62 ± 0.00</b>	<b>214.21 ± 0.00</b>	<b>96.05 ± 0.00</b>	<b>6.75 ± 0.00</b>

Table A4: Avg. wait time for various scenarios observed during training. Our method is also advantageous for wait time.

# scenarios	Chosen scenarios	Metrics			Improvement in %
		Trip Time	Delay	Wait	
1	<i>Ingolstadt21</i>	499.22 ± 8.02	387.37 ± 0.77	310.87 ± 5.43	-
3	<i>Ingolstadt21</i> + <i>Cologne8, Arterial 4×4</i>	351.84 ± 0.00	252.09 ± 0.00	166.67 ± 0.00	<b>+36.94%</b> w.r.t one scenario only
5	<i>Ingolstadt21</i> + <i>Cologne8, Arterial 4×4</i> + <i>Grid4×4, Grid5×5</i>	309.99 ± 0.00	185.53 ± 0.00	127.70 ± 0.00	<b>+49.64%</b> w.r.t one scenario only
7	<i>Ingolstadt21</i> + <i>Cologne8, Arterial 4×4</i> + <i>Grid4×4, Grid5×5</i> + <i>Fenglin, Nanshan</i>	278.05 ± 0.00	160.39 ± 0.00	96.05 ± 0.00	<b>+57.33%</b> w.r.t one scenario only

Table A5: Results of co-training with different numbers of scenarios based on *Ingolstadt21*.

# scenarios	Chosen scenarios	Metrics			Improvement in %
		Trip Time	Delay	Wait	
1	<i>Arterial 4×4</i>	403.16 ± 0.00	778.93 ± 0.00	259.19 ± 0.00	-
3	<i>Arterial 4×4</i> + <i>Cologne8, Ingolstadt21</i>	396.80 ± 0.00	767.22 ± 0.00	242.16 ± 0.00	<b>+3.22%</b> w.r.t one scenario only
5	<i>Arterial 4×4</i> + <i>Cologne8, Ingolstadt21</i> + <i>Grid4×4, Grid5×5</i>	388.02 ± 0.00	745.49 ± 0.00	217.38 ± 0.00	<b>+8.06%</b> w.r.t one scenario only
7	<i>Arterial 4×4</i> + <i>Cologne8, Ingolstadt21</i> + <i>Grid4×4, Grid5×5</i> + <i>Fenglin, Nanshan</i>	349.60 ± 0.00	697.79 ± 0.00	214.21 ± 0.00	<b>+13.68%</b> w.r.t one scenario only

Table A6: Results of co-training with different numbers of scenarios based on *Arterial 4×4*.

brought a performance boost to our method.

Table A8 illustrates the impact of various history lengths of the Upper Transformer on the results. A noteworthy enhancement in results occurs from  $K=10$  to  $K=20$ . Furthermore, an improvement is observed in scenarios featuring complex and large traffic flow (*Grid 5 × 5* and *Arterial 4 × 4*) when transitioning from  $K=20$  to  $K=30$ , whereas simpler scenarios show relatively minor changes. We also measured the average inference time for each model in *Grid5 × 5*. We use GPU(NVIDIA A800) for inference, in each time step Ours<sub>10</sub> costs 0.0208s, Ours<sub>20</sub> costs 0.0230s, Ours<sub>30</sub> costs 0.0255s.

Scenarios	Metrics	Ours	w/o Residual Link	w/o Dynamic Predictor	w/o Upper Transformer	w/o Lower Transformer
<i>Grid4×4</i>	Trip Time	162.47 ± 0.00	164.52 ± 0.00	164.27 ± 0.00	164.32 ± 0.00	164.18 ± 0.00
	Delay	50.27 ± 0.00	52.79 ± 0.00	52.44 ± 0.20	51.58 ± 0.00	52.42 ± 0.00
	Wait	24.57 ± 0.00	26.45 ± 0.00	25.97 ± 0.00	27.45 ± 0.00	26.33 ± 0.00
<i>Grid5×5</i>	Trip Time	220.63 ± 0.00	225.05 ± 0.00	232.75 ± 0.00	229.96 ± 0.00	226.43 ± 0.00
	Delay	187.74 ± 0.00	207.2 ± 0.00	198.54 ± 0.00	193.21 ± 0.00	208.65 ± 0.00
	Wait	79.62 ± 0.00	82.32 ± 0.00	90.46 ± 0.00	79.95 ± 0.00	84.89 ± 0.00
<i>Arterial4×4</i>	Trip Time	349.60 ± 0.00	354.99 ± 2.95	350.11 ± 0.00	382.14 ± 2.54	395.90 ± 0.00
	Delay	697.79 ± 0.00	768.57 ± 14.47	739.1 ± 0.00	723.87 ± 0.00	785.72 ± 0.00
	Wait	214.21 ± 0.00	201.22 ± 0.15	185.4 ± 0.00	206.38 ± 0.0	223.02 ± 0.0
<i>Ingolstadt21</i>	Trip Time	278.05 ± 0.00	283.89 ± 0.00	319.61 ± 17.09	296.74 ± 0.00	313.39 ± 0.00
	Delay	160.39 ± 0.00	176.22 ± 0.00	196.56 ± 0.00	172.63 ± 0.00	202.80 ± 0.00
	Wait	96.05 ± 0.00	99.45 ± 0.00	128.6 ± 15.56	105.25 ± 1.21	125.82 ± 0.00
<i>Cologne8</i>	Trip Time	88.55 ± 0.00	89.67 ± 0.00	88.98 ± 0.00	89.33 ± 0.00	90.11 ± 0.00
	Delay	24.31 ± 0.00	25.40 ± 0.00	24.91 ± 0.00	25.62 ± 0.22	26.36 ± 0.00
	Wait	6.75 ± 0.00	7.05 ± 0.28	7.01 ± 0.00	6.83 ± 0.14	7.61 ± 0.00
Avg. Decline ratio		-	4.07%	7.12%	4.25%	10.39%

Table A7: The detailed results of ablation studies reveal that each component contributes to improvement, showcasing the effectiveness of our design components.

Methods	Avg. Trip Time (seconds)					Avg. Delay Time (seconds)				
	Grid4×4	Grid5×5	Arterial4×4	Ingolstadt21	Cologne8	Grid4×4	Grid5×5	Arterial4×4	Ingolstadt21	Cologne8
Ours <sub>10</sub>	162.71 ± 0.00	223.12 ± 0.00	374.85 ± 0.87	283.02 ± 0.45	88.61 ± 0.00	50.69 ± 0.00	188.74 ± 0.00	725.06 ± 0.00	169.59 ± 2.37	24.41 ± 0.00
Ours <sub>20</sub>	<b>162.47 ± 0.00</b>	<u>220.63 ± 0.00</u>	<u>349.60 ± 0.00</u>	<u>278.05 ± 0.00</u>	<b>88.55 ± 0.00</b>	<b>50.27 ± 0.00</b>	187.74 ± 0.00	<u>697.79 ± 0.00</u>	<b>160.39 ± 0.00</b>	<b>24.31 ± 0.00</b>
Ours <sub>30</sub>	<u>162.57 ± 0.00</u>	<b>219.7 ± 0.00</b>	<b>345.88 ± 0.00</b>	<b>276.06 ± 0.00</b>	88.58 ± 0.00	50.92 ± 0.00	<b>181.21 ± 0.00</b>	<b>517.25 ± 0.00</b>	<u>162.79 ± 0.00</u>	<u>24.39 ± 0.00</u>

Table A8: The ablation studies of different history lengths of Upper Transformer. A noteworthy enhancement in results occurs from K=10 to K=20. In complex scenarios, K=30 can continue to bring improvements, whereas simpler scenarios show relatively minor changes.

## G More visualization attention weights of the Lower Transformer

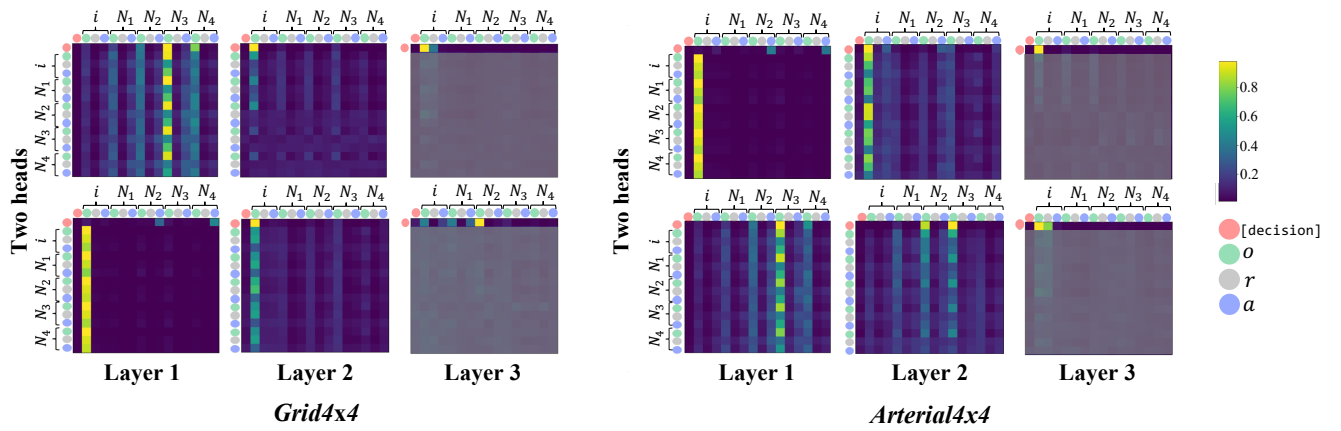


Figure A3: Visualizing Lower Transformer's attention in *Grid 4 × 4* and *Arterial 4 × 4* scenarios.